CHEMISTRY
A EUROPEAN JOURNAL

DOI: 10.1002/chem.200601334

Protein Recognition of Nickel–Cyclam Antiviral Complexes

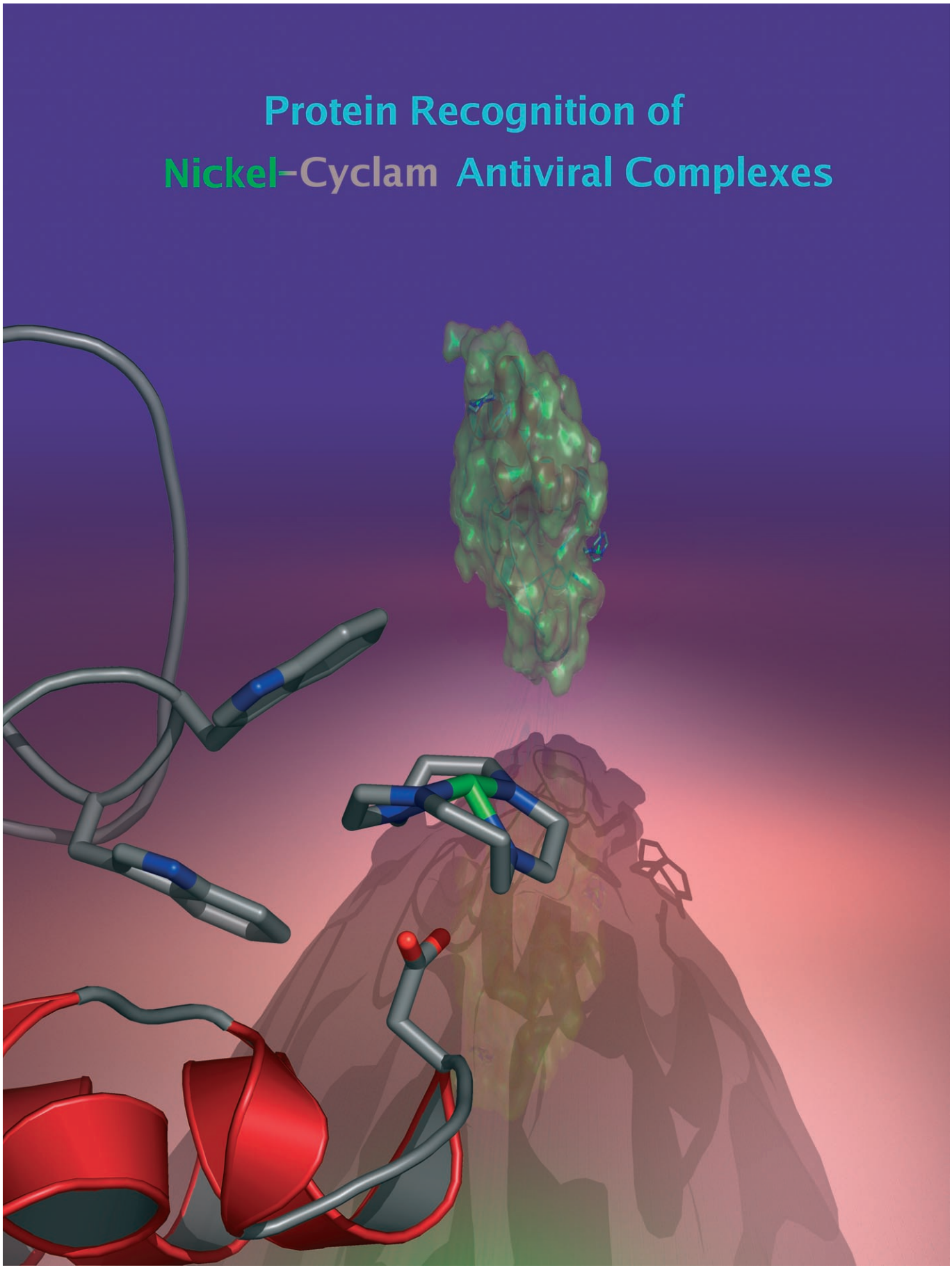

VIP

Configurations of Nickel–Cyclam Antiviral Complexes and Protein Recognition

Tina M. Hunter,[a] Iain W. McNae,[b] Daniel P. Simpson,[a] Alison M. Smith,[a] Stephen Moggach,[a] Fraser White,[a] Malcolm D. Walkinshaw,[b] Simon Parsons,[a] and Peter J. Sadler*[a]

Abstract: Nickel(II)–xylylbicyclam is a potent anti-HIV agent and binds strongly to the CXCR4 co-receptor. We have investigated configurational equilibria of Ni^{II}–cyclam derivatives, since these are important for receptor recognition. Crystallographic studies show that both *trans* and *cis* configurations are readily formed: [Ni(cyclam)-$(OAc)_2$]·H_2O adopts the *trans*-III configuration with axial monodentate acetates, as does [Ni(benzylcyclam)$(NO_3)_2$] with axial nitrate ligands, whereas [Ni(benzylcyclam)(OAc)](OAc)·2H_2O has an unusual folded *cis*-V configuration with Ni^{II} coordination to bidentate acetate. UV/Vis and NMR studies show that the octahedral *trans*-III configuration slowly converts to square-planar *trans*-I in aqueous solution. For Ni^{II}–xylylbicyclam, a mixture of *cis*-V and *trans*-I configurations was detected in solution. X-ray diffraction studies showed that crystals of lysozyme soaked in Ni^{II}–cyclam or Ni^{II}_2–xylylbicyclam contain two major binding sites, one involving Ni^{II} coordination to Asp101 and hydrophobic interactions between the cyclam ring and Trp62 and Trp63, and the second hydrophobic interactions with Trp123. For Ni^{II}–cyclam bound to Asp101, the *cis*-V configuration predominates.

Keywords: bioinorganic chemistry · coordination modes · macrocyclic ligands · nickel · protein recognition

Introduction

Cyclam (1,4,8,11-tetraazacyclodecane, Figure 1) and its derivatives are used in a wide range of applications, for example, catalysts, selective metal recovery agents, and as MRI contrast agents.[1] There is also current interest in xylylbicyclam ([1,4-phenylenebis-(methylene)]-bis-1,4,8,11-tetraazacyclotetradecane, AMD3100, Mozobil, Figure 1), a drug currently in clinical trials for mobilisation of stem cells to restore the immune systems of cancer patients whose immune systems have been compromised by previous treatments.[2] The drug has also been in clinical trials for the treatment of

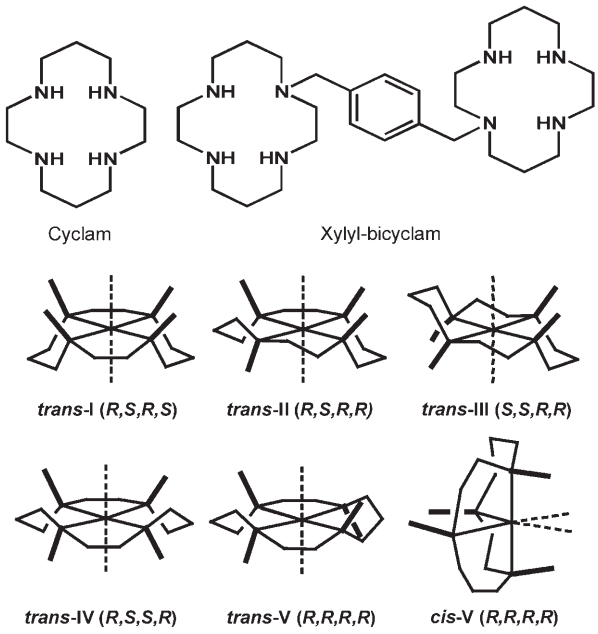

Figure 1. Structures of cyclam and xylyl bicyclam, along with common configurations of metal–cyclam complexes.

[a] T. M. Hunter, D. P. Simpson, A. M. Smith, S. Moggach, F. White, Dr. S. Parsons, Prof. Dr. P. J. Sadler
School of Chemistry, University of Edinburgh
West Mains Road, Edinburgh EH9 3JJ (UK)
Fax: (+44) 131-650-6452
E-mail: p.j.sadler@ed.ac.uk

[b] Dr. I. W. McNae, Prof. Dr. M. D. Walkinshaw
Institute of Cell and Molecular Biology
Michael Swann Building, University of Edinburgh
Mayfield Road, Edinburgh EH9 3JR (UK)

Supporting information for this article is available on the WWW under http://www.chemeurj.org/ or from the author.

HIV.[3,4] Xylylbicyclam has been shown to be a highly selective antagonist for the CXCR4 co-receptor protein, which is used by HIV to enter human T cells.[5] CXCR4 is a 7-helix trans-membrane receptor, involved in cell signalling and migration through chemokine binding.

The macrocycle cyclam is flexible enough to accommodate a wide range of metals.[6] The anti-HIV activity of xylylbicyclam is dependent on metal complexation in the following way:[7]

$$Zn_2 > \text{xylylbicyclam} = Ni_2 > Cu_2 > Co_2 \gg > Pd_2$$

Antiviral activity correlates with the strength of binding to the CXCR4 co-receptor. Upon metal complexation, five *trans* (planar) configurational isomers are possible (Figure 1).[8,9] Those that are symmetrical about their diagonal can fold to form *cis* configurations. Studies of the Cambridge Structural Database (CSD) show that the *trans*-III configuration is the most common configuration in the solid state.[10] It has been shown that *trans*-III complexes of zinc–cyclam complexes (with acetate, phthalate, perchlorate or chloride as counterions) equilibrate over a period of hours to form mixtures of *cis*-V, *trans*-I and *trans*-III isomers.[11,12] Acetate, in particular, can induce formation of the *cis*-V configuration, and the most prominent adduct of Zn^{II}_2–xylylbicyclam in the presence of acetate adopts *cis*-V/*trans*-I configurations.[12]

Metal complexes of xylylbicyclam appear to bind to the carboxylate groups of Asp262, Glu288 and Asp171 of CXCR4.[13] It has also been shown that metals can enhance the strength of binding of xylylbicyclam to the CXCR4 receptor in the following order: $Ni^{2+} > Zn^{2+} > Cu^{2+}$.[13] In our model of CXCR4 containing bound *cis*-V/*trans*-I Zn_2–xylylbicyclam, the *cis*-V ring is involved in direct bidentate binding to the oxygen atoms of the carboxylate side chain of Asp262, and forms double cyclam–NH hydrogen bonds to the carboxylate oxygen of Glu288.[12] Zinc in the *trans* ring can have axial coordination to a carboxylate oxygen of Asp171. Hydrophobic interactions between the cyclam backbone and the indole rings of tryptophan side chains (Trp95 and Trp283) located at each end of the zinc bicyclam binding site on CXCR4 may also play important roles in the receptor recognition process. These types of interactions were observed in our NMR and X-ray studies of Cu^{2+}–(bi)cyclam–lysozyme complexes.[14] Since nickel has been shown to enhance co-receptor binding of xylylbicyclam by a factor of 50 relative to the metal-free bicyclam, it is important to elucidate the configurational equilibrium of Ni^{2+}–(bi)cyclam complexes and their protein recognition properties.[13] So far, little is known about possible modes of coordination of nickel macrocycles to proteins, and to the CXCR4 receptor in particular. In this study we have investigated the configurations of nickel–cyclam, nickel–benzylcyclam and nickel–xylylbicyclam complexes, both in the solid state and in solution, and have probed protein interactions by studies of adducts with lysozyme both in solution and in crystals.

Results

X-ray Crystallography: Benzylcyclam (**1**), [Ni(cyclam)-$(OAc)_2$]·H_2O (**2**), [Ni(benzylcyclam)(OAc)](OAc)·2H_2O (**5**) and [Ni(benzylcyclam)$(NO_3)_2$] (**6**) were characterised by X-ray crystallography. Details of crystal packing are in the Supporting Information (Figures S1–S4). Benzylcyclam (**1**) crystallised as a neutral molecule (Figure 2). Two of the NH

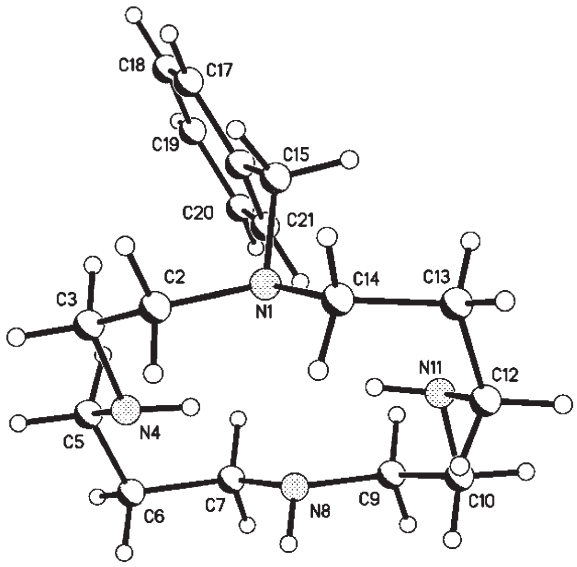

Figure 2. X-ray crystal structure of **1**, benzylcyclam, including the atom-numbering scheme.

hydrogen atoms point towards the centre of the macrocycle cavity, and are involved in hydrogen bonding to lone pairs on the opposite nitrogen atoms, with bond lengths of 2.272 and 2.394 Å. The hydrogen bond to the nitrogen with the benzyl substituent is significantly longer than the other, probably due to repulsions between the benzyl arm and the opposite side of the ring. The macrocycle appears to adopt a pseudo *trans*-III configuration. The aromatic ring is not involved in π–π stacking interactions (Figure S1).

The crystal structure of complex **2** consists of [Ni(cyclam)-$(OAc)_2$] species with the cyclam backbone in the octahedral *trans*-III configuration (Figure 3). These units are linked together by a network of hydrogen bonds involving water molecules (one per [Ni(cyclam)$(OAc)_2$] unit). Monodentate acetate occupies each axial coordination position on nickel with a Ni–O bond length of 2.1061(12) Å. These acetate groups form intramolecular hydrogen bonds to one of the NH groups on the cyclam ring (2.11 Å, Figure S2). This occurs on both faces of the ring, and hence stabilises this configuration. The water molecules form hydrogen bonds to the acetate ligands.

Complex **5** consists of units of $[Ni(benzylcyclam)(OAc)]^+$ with the cyclam backbone in the unusual *cis*-V configuration (Figure 4). The acetate group is bound to the metal in a bidentate manner, with Ni–O bond lengths of 2.1118(13) Å

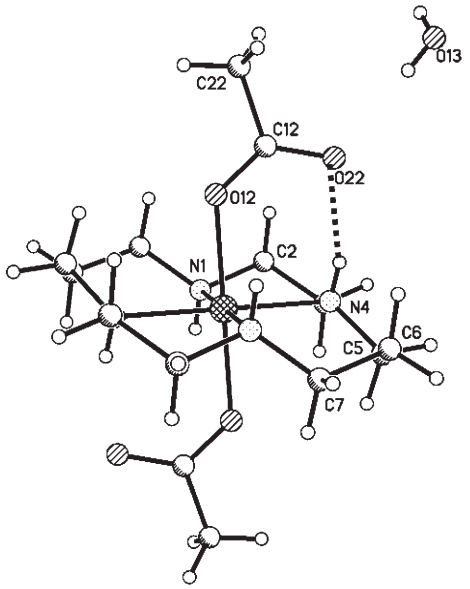

Figure 3. X-ray crystal structure of complex **2**, $[Ni(cyclam)(OAc)_2]\cdot H_2O$, including the atom-numbering scheme. The dotted line indicates a hydrogen bond between N4H and O22.

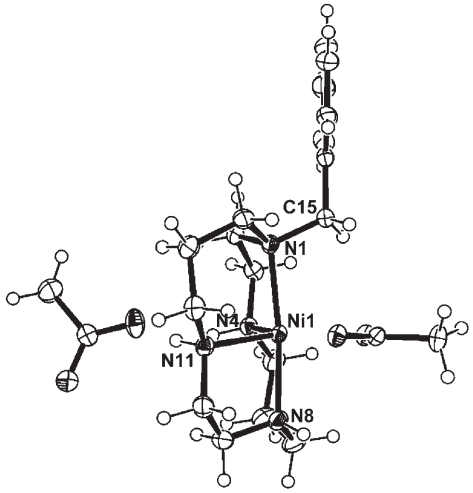

Figure 4. X-ray crystal structure of complex **5**, [Ni(benzylcyclam)(OAc)]-(OAc).$2H_2O$, including the atom-numbering scheme. The macrocycle is in the *cis*-V configuration, with one bidentate acetate bound to nickel. For clarity, the bonds between the acetate oxygen atoms and the nickel are omitted (shown in Figure S3 in the Supporting Information).

and 2.1534(13) Å. The acetate counterion is involved in hydrogen bonding to one of the NH groups of the cyclam ring, with NH–O hydrogen bonds of 2.069 Å and 1.995 Å. However, unusually, only one oxygen atom from uncoordinated acetate is involved in hydrogen bonding to the two NH groups. The other oxygen atom from this acetate is involved in a network of hydrogen bonds involving co-crystallised water molecules (Figure S3).

Complex **6** crystallised as $[Ni(benzylcyclam)(NO_3)_2]$ units, with the macrocycle in the *trans*-III configuration, and monodentate nitrate groups coordinated to nickel in the axial positions with Ni–O bond lengths of 2.173(2) Å and 2.166(2) Å (Figure 5). There is an internal hydrogen bond between one nitrate oxygen atom and a cyclam ring NH (NH-O = 2.059 Å and 2.209 Å, Figure S4). There are four molecules in the unit cell.

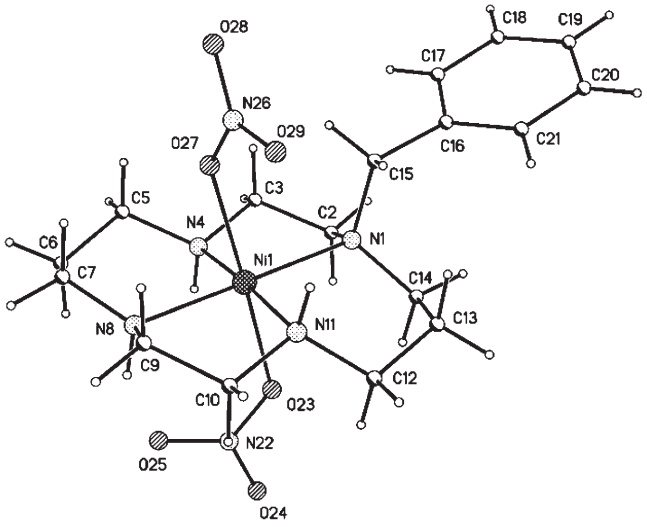

Figure 5. X-ray crystal structure of complex **6**, $[Ni(benzylcyclam)(NO_3)_2]$ including the atom-numbering scheme. The macrocycle is in the *trans*-III configuration, with nitrate directly bound to nickel.

A comparison of key bonds lengths and angles of the nickel complexes **2**, **5** and **6** is shown in Table 1. It can be seen that the Ni–N1 bond (the bond to the N bearing the benzyl substituent) is longer in the Ni^{II}–benzylcyclam complexes (2.1899(17) Å in **5** and 2.134(3) Å in **6**) relative to $[Ni(cyclam)(OAc)_2]$ complex (2.0678 Å).

Table 1. Selected bond lengths [Å] and angles [°] for nickel complexes.

	2	**5**	**6**
Ni–N1	2.0746(15)	2.1899(17)	2.134(3)
Ni–N4	2.0678(14)	2.0692(16)	2.046(3)
Ni–N8	2.0746(15)	2.1071(18)	2.073(3)
Ni–N11	2.0678(14)	2.0757(16)	2.049(3)
N1-Ni-N4	94.49(6)	84.21(6)	85.92(10)
N4-Ni-N8	85.51(6)	91.40(7)	94.04(11)
N8-Ni-N11	94.49(6)	83.52(7)	85.40(10)
N1-Ni-N11	85.51(6)	92.58(6)	94.68(10)
N4-Ni-N11	180.0(7)	100.36(6)	175.30(10)
N1-Ni-N8	180.0(7)	173.54(6)	179.48(11)

NMR studies of Ni^{II}–cyclam complexes: The 1D spectra of $[Ni(cyclam)(OAc)_2]$ (**2**), $Ni(cyclam)Cl_2$ (**3**) and $Ni(cyclam)(NO_3)_2$ (**4**) (recorded one week after dissolution to allow equilibria to be reached) showed a mixture of sharp and broad peaks. The 1D ^1H NMR spectrum of complex **2**, recorded in 90% H_2O/10% D_2O at 298 K, is shown in Figure S5 in the Supporting Information. The broad shifted peaks can be attributed to one or more paramagnetic forms

of the complex. Nickel(II) complexes ($3d^8$) can commonly exist as octahedral, paramagnetic species, or square-planar, diamagnetic species. Peaks from paramagnetic species are usually found between $\delta = -50$ and $+150$ ppm and peaks for diamagnetic complexes were observed between $\delta = 1$ and 4 ppm. The chemical shifts are summarised in Tables 2 and Table 3. Peaks shifted over a similar range have previously been reported for paramagnetic Ni^{II} octahedral complexes containing benzimidazole and pyridine ligands.[15]

Table 2. ^{1}H NMR chemical shifts [ppm] for paramagnetic nickel(II)–cyclam complexes (5 mM, 90% H_2O, 10% D_2O at 298 K).

Peak	δ [^{1}H]		
	2[a]	**3**	**4**
a	113.8	54.7	55.2
b	63.0	19.0	18.6
c	21.5	8.7	8.7
d	9.6	−0.3	−0.3
e	−0.6	−3.2	−3.2
f	−3.1		−52.6

[a] The peaks for complex **2** are labelled in Figure S5 in the Supporting Information.

The 1D and 2D homo- and heteronuclear NMR spectra of complex **2** in 90% H_2O/10% D_2O allowed a full assignment of the peaks for the diamagnetic form of this complex. The 2D [^{1}H,^{13}C] NMR spectrum showed peaks for six non-equivalent protons and three corresponding non-equivalent carbon atoms (Figure S6 in the Supporting Information). This shows that only one diamagnetic isomer was present in which cyclam adopts a symmetrical configuration. The 2D [^{1}H,^{1}H] COSY and TOCSY spectra were used to characterise the configuration fully. The [^{1}H,^{1}H] TOCSY NMR spectrum showed the presence of only one diamagnetic spin system, supporting the presence of only one isomer. The ^{1}H NMR peaks at $\delta = 1.32$ and 1.98 ppm both have the same ^{13}C shift ($\delta = 28.7$ ppm) and are assigned as the $CH_2CH_2CH_2$ protons. The signal at $\delta = 1.32$ ppm gives a cross-peak in the 2D [^{1}H,^{1}H] COSY NMR spectrum to the signal at $\delta = 3.20$ ppm (^{13}C $\delta = 50.7$ ppm), and hence is assigned as one of the $CH_2CH_2CH_2$ protons (Figure S6). The second ^{1}H NMR peak from this methylene group was located in the 2D [^{1}H,^{13}C] HSQC NMR spectrum at $\delta = 2.76$ ppm. As there were only three pairs of signals in the 2D [^{1}H,^{13}C] HSQC NMR spectrum, the remaining pair of ^{13}C signals at $\delta = 53.0$ ppm (^{1}H $\delta = 2.69$ and 2.53 ppm) were assigned as the CH_2CH_2 protons. It is known that only the *trans*-I and *trans*-III configurations give rise to three pairs of signals in the 2D [^{1}H,^{13}C] HSQC spectrum, therefore Ni^{II} cyclam acetate must adopt one of these configurations.[11] Since square-planar Ni^{II} is a better fit for the cavity in *trans*-I cyclam, it is concluded that diamagnetic Ni^{II} cyclam adopts the *trans*-I configuration in the present case.

On addition of two and ten molar equivalents of Na(OAc) to the solution of **2**, the ^{1}H NMR signal at $\delta = 1.9$ ppm increased in intensity and was therefore assigned to acetate. The signal is quite broad, suggesting that acetate is in fast exchange between bound and free forms. Little change in the rest of the spectrum was observed.

2D [^{1}H,^{1}H] COSY, TOCSY and NOESY NMR spectra of Ni^{II} cyclam complexes **3** and **4** showed that only one diamagnetic isomer was present in solution. The peak shifts were almost identical to those of complex **2**, and therefore it was concluded that complexes **3** and **4** are also in the *trans*-I configuration. The ^{1}H and ^{13}C NMR chemical shifts are listed in Table 2 and Table 3. The counterion (acetate, chloride or nitrate) has little effect on the overall structure of $[Ni(cyclam)]^{2+}$ in solution.

Solution studies of Ni^{II}–benzylcyclam complexes: [Ni(benzylcyclam)(OAc)](OAc) (**5**) was found to crystallise in the *cis*-V configuration. These crystals were then used for UV/Vis and NMR solution studies. The UV/Vis spectrum suggested that Ni^{II} coordination changed from octahedral (three absorption peaks in the UV/Vis spectrum, at 359, 459 and 556 nm) to square-planar (one absorption peak at 459 nm) slowly over a period of 40 h, and a colour change from purple to orange was observed (Figure S7 in the Supporting Information). The 1D ^{1}H NMR spectrum recorded 6 min after dissolution of the crystals showed a large number of broadened peaks from a paramagnetic species. However, over time, sharp peaks appeared in the region $\delta =$ 0–10 ppm. After 40 h, equilibrium was reached, and there was a mixture of sharp and broadened peaks present. The 2D [^{1}H,^{1}H] COSY, TOCSY and NOESY spectra along with a [^{1}H,^{13}C] HSQC NMR spectrum allowed a full assignment of the peaks from the diamagnetic species to be made. The NMR spectra were fully characterised as described in the Supporting Information (Figure S7). The 2D TOCSY NMR spectrum showed that there was only one diamagnetic isomer present. Key NOESY cross-peaks between the protons 5ax and 2b and between the protons 7ax and 10b suggested that this was a *trans*-I isomer, as these interactions would not be present in a *trans*-III configuration. The chemical shifts are listed in Table 4.

Complex **6** ([Ni(benzylcyclam)$(NO_3)_2$]) crystallised with the *trans*-III configuration. The crystals were purple. How-

Table 3. ^{1}H NMR chemical shifts [ppm] for diamagnetic nickel(II)–cyclam complexes (5 mM, 90% H_2O, 10% D_2O at 298 K).

		δ [^{1}H] and [^{13}C]									
		NCH_2CH_2N			$NCH_2CH_2CH_2N$			$NCH_2CH_2CH_2N$			NH
2	^{1}H ^{13}C ^{1}H	2.53	53.0	2.69	1.32	28.7	1.98	2.76	50.7	3.20	3.60
3	^{1}H ^{13}C ^{1}H	2.52	53.1	2.67	1.34	28.7	1.98	2.71	50.7	3.20	3.67
4	^{1}H ^{13}C ^{1}H	2.52	53.2	2.67	1.33	28.8	1.98	2.71	50.8	3.19	3.67

Table 4. ^{1}H and ^{13}C NMR chemical shifts (δ [ppm]) for diamagnetic nickel(II)–benzylcyclam complexes **5** [Ni(benzylcyclam)(OAc)](OAc)·2H_2O and **6** [Ni(benzylcyclam)$(NO_3)_2$] (5 mM, 90% H_2O, 10% D_2O at 298 K), with the atom-labelling scheme shown.

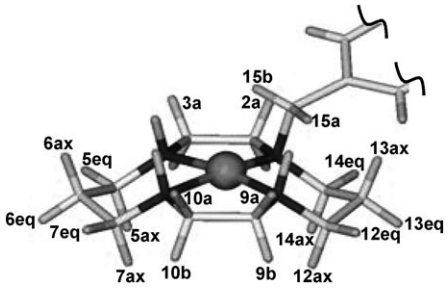

	5		6	
Atom	δ [^{1}H]	δ [^{13}C]	δ [^{1}H]	δ [^{13}C]
2a	2.68	59.0	2.67	59.0
2b	2.49		2.49	
3a	2.74	51.8	2.72	51.7
3b	2.67		2.66	
5ax	3.31	51.3	3.29	51.2
5eq	2.70		2.64	
6ax	1.26	28.6	1.27	28.5
6eq	1.97		1.98	
7ax	3.07	50.7	3.08	50.7
7eq	2.73		2.67	
9a	2.77	53.2	2.76	53.1
9b	2.62		2.60	
10a	2.84	53.3	2.82	53.3
10b	2.54		2.53	
12ax	3.66	51.4	3.64	51.3
12eq	2.92		2.86	
13	2.08	25.9	2.07	25.8
14ax	3.50	58.2	3.49	58.2
14eq	2.76		2.71	
15a	4.61	59.3	4.60	59.3
15b	3.68		3.67	

ever, upon dissolution in water, an immediate orange colour was observed. UV/Vis studies showed the rapid disappearance of the three peaks assigned to an octahedral species (359, 460 and 566 nm), with the rapid appearance of a band at 460 nm, assignable to a square-planar species. The reaction reached completion in about 4.3 h at 298 K. NMR studies also showed the formation of a square-planar diamagnetic species, but the presence of broad peaks showed that there was still some of the paramagnetic species present. The [^{1}H,^{13}C] 2D NMR spectrum of the final diamagnetic product was very similar to that of complex **5**, and hence it was assigned a *trans*-I configuration.

NMR studies of Ni_2(xylylbicyclam)$(OAc)_4$ (7): The 1D ^{1}H NMR spectrum for nickel(II)–xylylbicyclam acetate in 90% H_2O/10% D_2O is complicated (Figure S8). It is likely that there is a large number of species present in solution, a mixture of paramagnetic and diamagnetic arising from the possibility that two cyclam rings in the xylylbicyclam adducts may adopt different configurations and contain either paramagnetic or diamagnetic Ni^{II}. Spectra were recorded over a spectral width of $\delta = -400$ to $+400$ ppm, and the chemical shifts of the peaks observed between $\delta = -20$ and 250 ppm are listed in Table 5. A detailed analysis of peaks was not carried out, but it is evident by comparison with the ^{1}H NMR spectrum of complex **5**, [Ni(benzylcyclam)(OAc)](OAc), which also contains broad peaks at $\delta = -18.2$, -15.5 and -7.5 ppm, that compound **7** can also adopt the *cis*-V configuration in solution (Figure 6).

Table 5. ^{1}H NMR chemical shifts (δ [ppm]) for paramagnetic Ni_2(xylylbicyclam)$(OAc)_4$ (complex **7**, 5 mM, 90% H_2O, 10% D_2O at 298 K).

Peak	δ [^{1}H]	Peak	δ [^{1}H]
1	−18.2	8	69.7
2	−15.5	9	80.3
3	−7.5	10	117.7
4	11.7	11	169.0
5	13.3	12	191.8
6	21.4	13	211.8
7	42.1	14	245.5

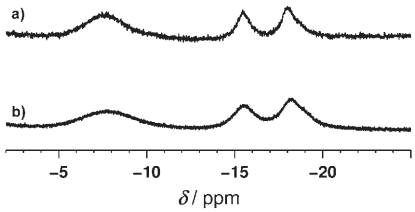

Figure 6. Part of the 1D ^{1}H NMR spectra of a) [Ni(benzylcyclam)(OAc)](OAc)·2H_2O, complex **5** and b) Ni_2(xylylbicyclam)$(OAc)_4$, complex **7**, at 298 K, showing the similarities of the peaks in the region of $\delta = -2$ to -30 ppm. Complex **6** gave rise to no peaks in this region.

Interactions of nickel–cyclam with lysozyme: [Ni(cyclam)$(OAc)_2$] (**2**) was added to a solution of lysozyme (HEWL from egg white) at pH 4.5 in 90% H_2O/10% D_2O to give molar ratios of **2**/lysozyme of 1, 5 or 10:1. The main features of the 1D ^{1}H NMR spectrum of HEWL were unchanged after addition of up to ten molar equivalents of the nickel complex (Figure S9), which indicated that the interaction had little effect on the overall protein fold. In this case, the solution contained a mixture of paramagnetic and diamagnetic Ni–cyclam, as shown by the presence of sharp and broadened peaks in the 1D spectrum. Upon reaction of **2** with lysozyme, broadened peaks from paramagnetic Ni–cyclam were still observed at $\delta = 40.3$, 19.0, -8.4 and -18.1 ppm. However, specific ^{1}H NMR peaks from lysozyme broadened suggesting that binding to Ni^{II} had occurred. In the 1D ^{1}H NMR spectrum, resonances from lysozyme which broadened are assignable to Trp62 and Trp63. The resonances of Trp63 were the most affected, and the NH signal of Trp63 was too broad to observe in the 1D NMR spectrum after the addition of five or ten molar equivalents of the nickel complex. In the 2D [^{1}H,^{1}H] TOCSY NMR spectrum, the cross-peak from Hε^{1}/Hδ^{1} Trp63 disappeared upon the addition of one molar equivalent of **2** (Figure 7). This was the only significant change to the 2D

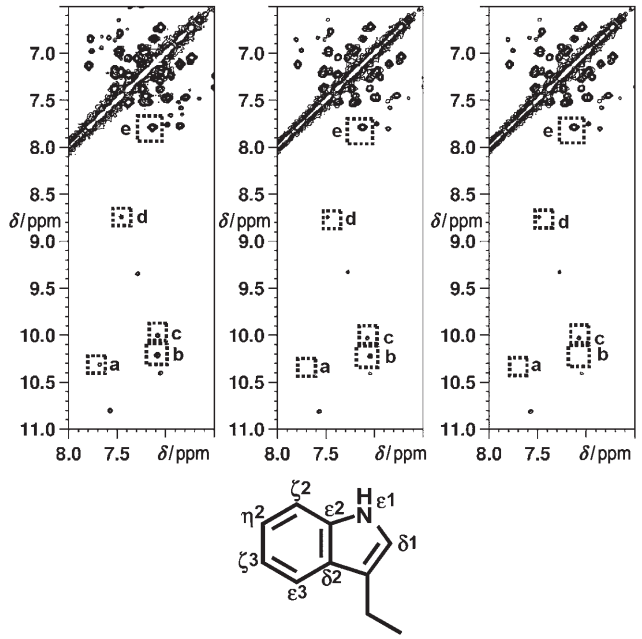

Figure 7. 2D [^{1}H,^{1}H] COSY NMR spectra of lysozyme in 90% H_2O/10% D_2O, before (left), after (middle) addition of one molar equivalent of [Ni(cyclam)$(OAc)_2$], and (right) addition of five molar equivalents of [Ni(cyclam)$(OAc)_2$]. The labelling Scheme for Trp is included. There was little further change in the 2D NMR spectrum after the addition of ten molar equivalents of [Ni(cyclam)$(OAc)_2$]. Trp assignments: a, Trp63 Hε^1/Hδ^1; b, Trp62 Hε^1/Hδ^1; c, Trp108 Hε^1/Hδ^1; d, His15 Hε^1/Hδ^2; e, Trp123 Hε^1/Hδ^1.

NMR spectrum after the addition of one molar equivalent of Ni-cyclam. However, following the addition of five molar equivalents, the Hε^1/Hδ^1 signal from Trp62 also disappeared.

Binding of nickel cyclams to lysozyme crystals: Lysozyme crystals were soaked in solutions of the Ni^{II}–cyclam complex **2** or Ni^{II}_2–bicyclam complex **7**. The positions of the nickel atoms in adducts of lysozyme with both complex **2** ([Ni(cyclam)$(OAc)_2$]) and complex **7** (Ni_2(xylylbicyclam)$(OAc)_4$) were unequivocally found as strong peaks in an $|F_o|-|F_c|$ map. These peaks were confirmed as resulting from the nickel atoms owing to their strong anomalous signal (data collected at K-edge wavelength). In the structures of the adducts of lysozyme with both the monocyclam and xylylbicyclam complexes, the Ni^{II} binding sites are similar and the same as those found previously for copper cyclams adducts, with two distinct binding sites.[14] These sites are on different regions of the protein, but are brought close together by crystal symmetry. The sites are shown in Figure 8. Site 1 is close to the side chain of Asp101, while site 2 is closest to the side chain of Trp123. Site 1 involves hydrophobic stacking interactions between the cyclam backbone and two tryptophan residues, Trp62 and Trp63, and also direct binding of the Ni to the carboxylate group of Asp101. There is a water molecule occupying the second axial position on the nickel atom. The second site involves stacking interactions between the cyclam ring and Trp123. Although the nickel sites can be unequivocally positioned, the exact cyclam ring configuration is less well defined; this fact probably indicates the presence of a mixture of configurations. It is apparent that in site 2 the majority of the cyclam rings adopt *trans* configuration in both the xylylbicyclam and monocyclam structures. In the Ni–xylylbicyclam structure, it is clear that the cyclam ring in site 1 is also in a *trans* configuration with the nickel interacting directly with the carboxylate side chain of Asp101 and the periphery of the cyclam ring is close to the indole rings of the side chains of Trp62 and Trp63. In the structure of the adduct that contains the nickel monocyclam complex, the cyclam ring in site 1 is predominately in the *cis* configuration. This is the same as previously found for copper cyclam adducts of lysozyme.[14] It is also apparent that the monocyclam in site 1 is a mixture of *cis* and *trans* configurations as evidenced by the shape of the electron density around the nickel position in the anomalous map.

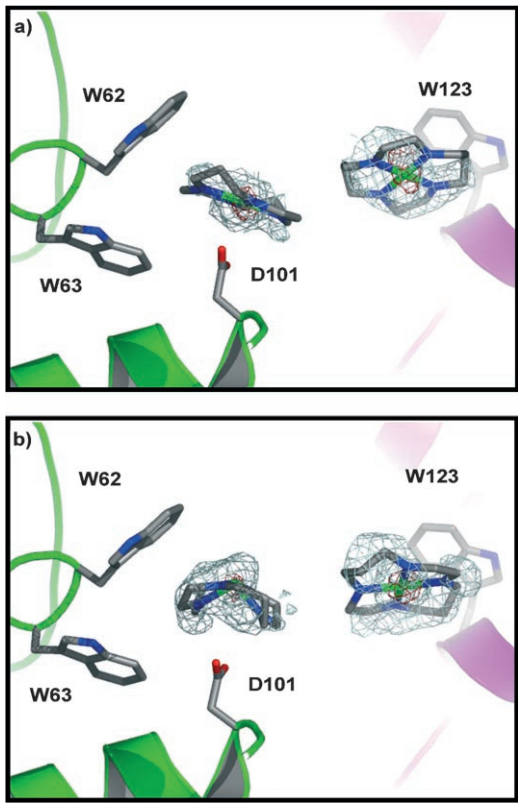

Figure 8. The two nickel bicyclam and monocyclam binding sites in HEWL crystals. a) The nickel bicyclam site, and b) nickel monocyclam site. Electron density is shown for 2|Fo|-|Fc| at 0.8 σ (blue) and for anomalous differences at 8 σ (red). In the case of Ni^{II} xylylbicyclam, the linker and second cyclam are not seen in the electron density map and are likely to be disordered. In each picture, site 1 is on the left and involves binding of Ni to the carboxylate group of Asp101 and hydrophobic interactions with Trp62 and Trp63, and site 2 is on the right and involves hydrophobic interactions with Trp123 (background). The two sites lie between lysozyme molecules in the crystal and are ca. 5 Å apart. (In figure, W = Trp, D = Asp.)

It is also apparent from the anomalous peaks that there is a third nickel site in the adduct that contains nickel–xylylbicyclam. This nickel atom in this site is not associated with a cyclam ring, but is coordinated to the carboxylate group of

Asp52 and water molecules. This indicates the presence of free nickel, which is perhaps a consequence of the low pH (4.5) of the crystallisation medium and high affinity of the Asp52 site.

Discussion

Three nickel–cyclam complexes were crystallised in this work. The [Ni(cyclam)$(OAc)_2$] diacetate complex (**2**) and the [Ni(benzylcyclam)$(NO_3)_2$] complex (**6**) both adopt the common *trans*-III configuration, while the [Ni(benzylcyclam)(OAc)](OAc) complex (**5**) has the *cis*-V configuration. Acetate was found to bind to nickel in both a mono- and a bidentate manner. Several X-ray crystal structures of nickel–cyclam complexes have previously been published. The majority (62) are in the *trans*-III configuration; however, there are seven *cis*-V structures and one *trans*-V structure in the CSD. The majority of the *cis*-V complexes contain chelating ligands. However, one complex, *cis*-[Ni(cyclam)$(H_2O)_2]^{2+}$, contains water molecules as the ligands directly bound to nickel.[16] This complex was made from $[Ni(cyclam)(en)]^{2+}$, which is locked into the *cis*-V configuration, by removal of the chelated en ligand under acidic conditions. However, in solution, *trans*-I, *trans*-III and *cis*-V isomers of $[Ni(cyclam)]^{2+}$ complexes have been observed.[9,17–19]

The work reported here shows that nickel–cyclam complexes can rapidly convert from paramagnetic *trans*-III to diamagnetic *trans*-I configurations in aqueous solution. However, if the cyclam backbone initially adopts the *cis*-V configuration, this too can convert to a *trans*-I configuration, but much more slowly. We did not attempt to make specific assignment for peaks of the paramagnetic species. The shifts result from both through-space (dipolar, pseudocontact, $\propto 1/r^3$) and through-bond (contact, delocalised unpaired spin density) effects. Soon after dissolution in water, the acetate Ni^{II}–benzylcyclam complex **5**, which has the *cis*-V configuration in the crystalline state, gave a similar set of peaks to those observed for Ni_2–xylylbicyclam (Figure 6). This suggests that Ni_2–xylylbicyclam can readily adopt *cis*-V configurations in solution. The *cis*-V configuration may be involved in the binding of metal cyclams to the CXCR4 co-receptor.[12] The ability to adopt a *cis*-V configuration may account for the high antiviral activity of nickel–xylylbicyclam, in contrast to Pd^{II}– and Co^{III}–cyclams. The chemistry of Pd^{II} is dominated by square-planar complexes and octahedral coordination is rare, whereas configurational interconversion (and axial ligand interconversion) of Co^{III} complexes is probably kinetically unfavourable. However, our data also suggest that the *cis*-V configuration of Ni^{II}–cyclam is not readily induced by binding to acetate, instead a stable square-planar *trans*-I configuration forms in solution over time. This is in contrast to the highly active zinc complex.[11,12] Acetate readily induces formation of *cis*-V configurations of zinc–cyclam and zinc–xylylbicyclam complexes. It is known that Ni^{II} but not Zn^{II} has a strong tendency to form square-planar complexes. Axial coordination to Ni^{II} and Zn^{II} for *trans*-III cyclams should also be favoured in protein complexes, but perhaps not to Pd^{II} and Co^{III}.

The counterion (acetate, Cl^-, or NO_3^-) appears to have little effect on the overall configuration of nickel–cyclams or nickel–benzylcyclams in solution. In contrast, aqueous solutions of zinc–cyclam perchlorate and zinc–cyclam chloride complexes consist mainly of the *trans*-III configuration, while carboxylato complexes predominantly adopt the *cis*-V configuration.[11]

The nickel–benzylcyclam nitrate complex **6** is unusual in that nitrate is involved in direct binding to the metal. Nitrate normally has a weak affinity for metals, and there are few examples of Ni^{II} complexes containing coordinated nitrate (none in the CSD). However, in solution nitrate appears to dissociate readily and an equilibrium between square-planar and octahedral species is rapidly formed.

There are only a few reported crystal structures of metal–benzylcyclam complexes, and only one of these has the *cis*-V configuration, [Pb(benzylcyclam)$(O_2NO)_2$], which contains eight-coordinate Pb^{2+}.[20] The Pb^{2+} ion is too big to fit into a planar (*trans*-I or *trans*-III) cyclam ring, and hence the ring folds and forms the *cis*-V configuration. In crystals of $[Cu^{II}(benzylcyclam)]^{2+}$, the cyclam backbone adopts the stable *trans*-III configuration.[21] Of the crystal structures of nickel–cyclam complexes in the CSD, 28 involve direct bonding between nickel and oxygen. The Ni–O bond lengths vary from 2.070 Å to 2.109 Å, and the Ni–N bond lengths vary from 1.963 Å to 2.109 Å.[22,23] The two nickel–benzylcyclam complexes crystallised here have one long Ni–N bond (2.1899(17) Å and 2.134(3) Å), involving the alkylated nitrogen atom. A similar increase in bond length is seen in [Cu(benzylcyclam)$(NO_3)_2$].[21]

The crystallisation studies show that planar *trans* configurations of Ni^{II}–cyclam readily bind to lysozyme. There is evidence at one site close to Asp101, that a *cis* configuration is involved in the binding, but only for nickel–cyclam, not for nickel–xylylbicyclam. In the case of the nickel–xylylbicyclam complex, there was evidence for occupation of a third Ni^{II} binding site, which appeared to only contain nickel and no cyclam, with octahedral coordination to Asp52 and water. Asp52 has been shown to be the binding site for free Ni^{II} in previous studies of lysozyme.[24,25] It is clear that the macrocycle itself directly influences the site of binding of Ni^{II} to the protein. In solution, our NMR studies show that paramagnetic nickel cyclam binds close to Trp62 and Trp63 residues that flank the Asp101 site and form hydrophobic contacts with the periphery of the nickel cyclam. Such a tryptophan sandwich has a parallel in some protein–protein complexes, for example, receptor–antibody complexes, in which a proline ring forms the filling in the sandwich. The similarity of the skeleton of a proline ring and segments of the cyclam macrocycle is evident. Since the NMR peaks of Trp123 are not significantly broadened, this suggests that Ni cyclam bound at this site is diamagnetic (square-planar, *trans*-I), consistent with the lack of axial ligands observed in the X-ray structure. Ni^{II}–cyclam and $Ni^{II}{}_2$–xylylbicyclam

bind to lysozyme in similar sites as Cu^{II}–cyclam and Cu^{II}_2–xylylbicyclam, confirming the role of the macrocycle as well as the metal in determining the binding site.[14]

Conclusion

The X-ray structures of [Ni(cyclam)$(OAc)_2$] (**2**), [Ni(benzylcyclam)(OAc)](OAc) (**5**) and [Ni(benzylcyclam)-$(NO_3)_2$] (**6**) showed that in the solid-state nickel–cyclam derivatives can adopt *trans*-III and *cis*-V configurations. However in solution the square-planar *trans*-I species is formed in all cases, as identified using 1D and 2D ^{1}H and ^{13}C NMR spectroscopy. Along with these diamagnetic square-planar *trans*-I species, octahedral paramagnetic species were also shown to exist in aqueous solution, by the presence of shifted, broadened peaks in ^{1}H NMR spectra. The 1D ^{1}H NMR spectrum of the Ni^{II} adduct of the anti-HIV drug xylylbicyclam (Figure S8 in the Supporting Information) is extremely complicated, due to the presence of many paramagnetic and diamagnetic species. However, the ^{1}H NMR spectrum of the *cis*-V acetate complex **5** (*cis*-V in the crystalline state) soon after dissolution showed presence of a *cis*-V species with similar shifts to those detected for one of the forms of Ni_2(xylylbicyclam)$(OAc)_4$ (**7**). The ability to form a *cis*-V isomer may enhance binding to the CXCR4 co-receptor and contribute to the anti-HIV activity of cyclam-based complexes. As for Cu^{II}–cyclam and Cu^{II}_2–xylylbicyclam, two binding sites were found for Ni^{II}–cyclam and Ni^{II}_2–xylylbicyclam in crystals of lysozyme. These involve direct coordination to aspartate carboxylate oxygen atoms, as well as hydrogen bonding and hydrophobic interactions with Trp rings. In the aspartate site, Ni–cyclam can readily form *cis*-V configurations, whereas the *trans*-I configuration appears to occur in the second site. Different macrocycle configurations are likely to be recognised differently by the CXCR4 receptor. The exploration of metallomacrocycles with constrained configurations may lead to optimisation of protein binding properties and of antiviral and stem-cell mobilising activity.

Experimental Section

Cyclam and hen egg white lysozyme (HEWL) were purchased from Sigma Aldrich. Xylylbicyclam and benzylcyclam were prepared by using a published method.[26]

Benzylcyclam (1): Crystals suitable for X-ray diffraction were grown by slow evaporation of a solution of **1** in methanol.

[Ni(cyclam)$(OAc)_2$]H_2O (2): Cyclam (400.85 mg, 2 mmol) was dissolved in methanol (50 mL) and Ni$(OAc)_2{\cdot}4H_2O$ (363.46 mg, 2 mmol) was added. The reaction was stirred overnight under N_2. The resulting purple solution was filtered and concentrated to dryness to give a purple powder. This powder was recrystallised by slow evaporation from methanol into diethyl ether to give [Ni(cyclam)$(OAc)_2$]H_2O, yield 56% (422 mg, 1.12 mmol). 600 MHz 1D and 2D NMR spectra (COSY, TOCSY, NOESY and [^{1}H,^{13}C] HSQC) of solutions of this product in 100% D_2O and 90% H_2O/10% D_2O were recorded (see Tables 2 and 3 for data). Selected IR (KBr): $\tilde{\nu}$ = 3528 (OH), 3457 (NH), 3246 (NH), 2939 (CH), 2875 (CH), 1636 (OH), 1571 (CO), 1406 cm^{-1} (CO); ES-MS: m/z: 376.9 $[M+H-H_2O]^+$, 316.8 $[M-OAc-H_2O]^+$, 256.7 $[M-2(OAc)-H_2O-H]^+$; elemental analysis calcd (%) for $C_{14}H_{32}N_4NiO_5$: C 42.56, N 14.18, H 8.16; found: C 42.15, N 14.19, H 7.84.

Ni(cyclam)Cl_2 (3): Cyclam (50.7 mg, 0.25 mmol) was dissolved in methanol (20 mL) and $NiCl_2{\cdot}6H_2O$ (59.74 mg, 0.25 mmol) was added. The reaction was stirred overnight under N_2. The resulting orange/brown solution was filtered and concentrated to dryness to give a purple powder, which was recrystallised from methanol, giving a purple precipitate, yield 77% (63.3 mg, 0.19 mmol). 1D and 2D NMR spectra (COSY, TOCSY, NOESY and [^{1}H,^{13}C] HSQC) were recorded on this product on a 600 MHz spectrometer in 90% H_2O/10% D_2O (see Tables 2 and 3 for data). Selected IR (KBr): $\tilde{\nu}$ = 3262 (NH), 3211 (NH), 2926 (CH), 2857 cm^{-1} (CH); ES-MS: m/z: 332.7 $[M+H]^+$, 292.6 $[M-Cl]^+$, 256.6 $[M-2Cl-H]^+$; elemental analysis calcd (%) for $C_{10}H_{24}N_4NiCl_2$: C 36.40, N 16.98, H 7.33; found: C 36.55, N 17.12, H 7.30.

Ni(cyclam)$(NO_3)_2$ (4): Cyclam (104.65 mg, 0.52 mmol) was dissolved in methanol (20 mL) and Ni$(NO_3)_2{\cdot}6H_2O$ (150.21 mg, 0.52 mmol) was added. The reaction was stirred overnight under N_2. The resulting orange solution was filtered and concentrated to dryness to give a purple powder, which was dried under high vacuum and recrystallised from methanol, yield 83% (140.4 mg, 0.43 mmol). 1D and 2D NMR spectra (COSY, TOCSY, NOESY and [^{1}H,^{13}C] HSQC) were recorded on this product on a 600 MHz spectrometer in 90% H_2O/10% D_2O (see Tables 2 and 3 for data). Selected IR (KBr): $\tilde{\nu}$ = 3261 (NH), 3212 (NH), 2927 (CH), 2871 (CH), 1381 cm^{-1} (NO); ES-MS: m/z: 319.7 $[M-NO_3]^+$, 256.7 $[M-2(NO_3)-H]^+$; elemental analysis calcd (%) for $C_{10}H_{24}N_6NiO_6$: C 31.36, N 21.94, H 6.32, found: C 31.25, N 22.21, H 6.28.

[Ni(benzylcyclam)(OAc)](OAc)·2H_2O (5): Benzylcyclam (48.9 mg, 0.17 mmol) was dissolved in methanol (10 mL) and Ni$(OAc)_2{\cdot}4H_2O$ (42.9 mg, 0.17 mmol) was added. The reaction was stirred overnight under N_2. The resulting purple solution was filtered and concentrated to dryness to give a purple powder, which was dried under high vacuum. The product was recrystallised from slow evaporation of a solution of **5** in methanol and diethyl ether to give purple crystals suitable for X-ray crystallography, yield 79% (62.1 mg, 0.13 mmol). 600 MHz 1D and 2D NMR spectra (COSY, TOCSY, NOESY and [^{1}H,^{13}C] HSQC) of this product 90% H_2O/10% D_2O were recorded (see Table 4 for data). ES-MS: m/z: 407.3 $[M-OAc]^+$, 347.3 $[M-2(OAc)-H]^+$; elemental analysis calcd (%) for $C_{10}H_{24}N_6NiO_6$: C 31.36, N 21.94, H 6.32; found: C 31.25, N 22.21, H 6.28.

[Ni(benzylcyclam)$(NO_3)_2$] (6): Benzylcyclam (100.1 mg, 0.345 mmol) was dissolved in methanol (10 mL) and Ni$(NO_3)_2{\cdot}6H_2O$ (100.2 mg, 0.345 mmol) was added. The reaction was stirred overnight under N_2. The resulting orange solution was filtered and concentrated to dryness to give a purple powder, which was dried under high vacuum. The product was recrystallised from slow evaporation of a solution of **6** in methanol and diethyl ether to give purple crystals suitable for X-ray crystallography, yield 63% (106.2 mg, 0.22 mmol). 600 MHz 1D and 2D NMR spectra (COSY, TOCSY, NOESY and [^{1}H,^{13}C] HSQC) of this product in 90% H_2O/10% D_2O were recorded (see Table 4 for data). ES-MS: m/z: 410.2 $[M-(NO_3)]^+$, 347.2 $[M-2(NO_3)-H]^+$

Ni_2(xylylbicyclam)$(OAc)_4$ (7): Ni$(OAc)_2{\cdot}4H_2O$ (11.1 mg, 0.04 mmol) was dissolved in methanol (5 mL) and added to a solution of xylylbicyclam (0.5 molar equiv, 11.2 mg, 0.02 mmol) in methanol (10 mL). The mixture was stirred and refluxed for 2 h. The solvent was then removed under reduced pressure and the resulting purple solid dried under vacuum. The product was dissolved in methanol and slow diffusion of diethyl ether produced a purple powder, yield 60% (10.3 mg, 0.012 mmol). 800 MHz 1D and 2D NMR spectra ([^{1}H,^{15}N] HSQC) of this product in 90% H_2O/10% D_2O were recorded (see Table 5 for data). Selected IR (KBr): $\tilde{\nu}$ = 3423 (NH), 2927 (CH), 2869 (CH), 1565 (CO), 1412 cm^{-1} (CO); ES-MS: m/z: 368.2 $[M-2OAc]^{2+}$, 368.2 $[M-3OAc-H]^{2+}$, 308.2 $[M-4OAc-2H]^{2+}$.

X-ray crystallography: All diffraction data on small molecules were collected by using $Mo_{K\alpha}$ radiation (λ = 0.71073 Å) on a Bruker Smart Apex CCD Diffractometer equipped with an Oxford Cryosystems low-temperature device operating at 150 K. Absorption corrections were carried out with the multi-scan procedure SADABS.[27] The crystal structures of **1**

Table 6. Crystal data and data collection for complexes **1**, **2**, **5** and **6**.

	1	**2**	**5**	**6**
formula	$C_{17}H_{30}N_4$	$NiC_{14}H_{32}N_4O_5$	$NiC_{21}H_{40}N_4O_6$	$NiC_{17}H_{30}N_6O_6$
M_r	290.45	395.15	503.28	473.18
crystal system	monoclinic	monoclinic	triclinic	triclinic
space group	C_2/c	C_2/c	$P\bar{1}$	$C\bar{1}$
Z	8	4	2	16
a [Å]	21.8452 (9)	13.1311 (5)	9.1602 (2)	15.1969 (4)
b [Å]	8.9562 (4)	12.5959 (5)	11.4196 (2)	54.4939 (14)
c [Å]	18.9669 (8)	11.6830 (5)	12.7686 (2)	10.1440 (3)
α [°]	90.00	90.00	93.3190 (10)	90.00
β [°]	113.205 (3)	99.906 (3)	110.9230 (10)	90.730 (2)
γ [°]	90.00	90.00	101.1570 (10)	90.00
V [Å^3]	3410.7 (3)	1903.54 (13)	1212.21 (4)	8400.00 (4)
T [K]	150	150	150	150
ρ_{cald} [g cm^{-3}]	1.131	1.379	1.379	1.497
μ [mm^{-1}]	0.069	1.049	0.843	0.971
unique reflections	4729	2584	6820	19658
measured reflns	20473	10647	20885	48982
$R1$ (obsvd reflns)	0.0498	0.0360	0.0480	0.0365
$wR2$ (all refl)	0.1082	0.0909	0.1072	0.0758

and **2** were solved using direct methods (SIR92[28] and SHELXS,[29] respectively), while those of **5** and **6** were solved by Patterson methods (DIRDIF).[30] The models were refined against F^2 using CRYSTALS[31] (**1**) or SHELXL[32] (**2**, **5** and **6**). Anisotropic displacement parameters were refined for all non-H atoms. Table 6 gives the crystal data and data collection parameters for complexes **1**, **2**, **5** and **6**.

For complex **1**, hydrogen atoms on N were located in a difference map and refined subject to similarity restraint on the three NH distances. For complex **5**, the hydrogen atoms on the water molecules were located in a difference map. The water molecules were thereafter treated as freely-rotating rigid bodies. Other hydrogen atoms were placed in calculated positions. For complex **2**, the Ni and the macrocyclic ligand occupy inversion centres, while the water resides on a twofold axis.

There are four molecules in the asymmetric unit of the crystal structure of **6**. The structure is twinned, and the unconventional $C\bar{1}$ setting was chosen to make the twin law more evident. The cell does not deviate significantly from metric monoclinic symmetry, and the constrained dimensions were used throughout the analysis. The twin law was taken to be twofold about [010]. The twin scale factor was 0.2668(7). The cell was actually metrically nearly orthorhombic, though there was no sign of further twinning about [100] or [001].

CCDC-621100 (**1**), CCDC-621101 (**2**), CCDC-621102 (**5**), and CCDC-621103 (**6**) contain the supplementary crystallographic data for this paper. These data can be obtained free of charge from The Cambridge Crystallographic Data Centre via www.ccdc.cam.ac.uk/data_request/cif.

NMR studies of lysozyme with [Ni(cyclam)(OAc)$_2$]·H$_2$O: All NMR experiments were performed on solutions containing 90% H_2O/10% D_2O. The water resonance was suppressed by presaturation. Standard pulse sequences were used for 2D TOCSY and COSY (mixing times of 60 and 80 ms, respectively). The pH of 5 mM solutions of HEWL used for NMR titrations was adjusted to 4.5 using 0.1 M HCl. Titrations were carried out by adding microlitre aliquots of aqueous [Ni(cyclam)(OAc)$_2$]·H_2O (125 mM, pH 4.55), adding 1, 5 and 10 molar equivalents.

Soaking of lysozyme crystals with nickel complexes: Lysozyme crystallisation was achieved by using the hanging drop vapour diffusion technique. The reservoir solution contained 100 μL of 50 mM acetate buffer, pH 4.5, 200 μL of saturated NaCl solution and 700 μL of distilled water. The hanging drop contained 2.5 μL of HEWL (50 mg mL^{-1} in acetate buffer) and 2.5 μL of the reservoir solution. Crystals suitable for X-ray diffraction grew within one week at 277 K.

Soaking was carried out for five days at 288 K with solid of either complex **2** or complex **7** being added directly to crystallisation drops in which crystals had formed until saturation was achieved. Soaked crystals were removed in a cryoloop and frozen in liquid nitrogen using type B immersion oil as a cryoprotectant.

Data collection was performed at station 10.1 (λ = 1.486) for the Ni–bicyclam complex and station 14.1 (λ = 1.488) for the Ni–cyclam complex, both stations at the Daresbury Synchrotron Radiation Source. Data processing and scaling was performed using the programs MOSFLM and SCALA[33] as part of the CCP4 program package.[34] The initial structure was solved by using the previously solved HEWL–CuCyclam structure (pdb id; 1YIK). Refinement was performed using the program REFMAC[35] with manual checking, correction and water addition being performed in the program COOT.[36] Data collection and refinement statistics are summarised in Table 7. The

Table 7. Crystal data for lysozyme crystals soaked with complex **2** and complex **7**.

	2	**7**
space group	$P4_32_12$	$P4_32_12$
$a=b$ [Å]	77.32	77.57
c [Å]	37.9480	38.3555
$\alpha=\beta=\gamma$ [°]	90	90
resolution range[a]	54.64–1.75 (1.84–1.75)	34.38 –1.75 (1.84–1.75)
molecules per asymm unit	1	1
observed reflections	192485	111437
unique reflections	12132	12329
mean [(I)/sd(I)][a]	25.5 (4.3)	16.8 (3.3)
completeness [%][a]	100 (99.8)	99.9 (100)
multiplicity[a]	15.9 (13.9)	9.0 (9.0)
anomalous completeness [%][a]	100 (99.9)	99.9 (100)
anomalous multiplicity[a]	8.6 (7.3)	4.9 (4.8)
R_{merge} [%][a]	8.3 (53.7)	9.0 (50.2)
Refinement		
R/R_{free} [%]	18.1/24.6	18.4/23.2
rms bonds [Å]	0.019	0.018
rms angles [°]	1.881	1.795
average isotropic B [Å^2]	20.845	25.685

[a] Numbers in parentheses refer to high shell.

structures of the lysozyme complexes have been deposited in the RCSB Protein Data Bank[37] assigned the codes 2H9K for the Ni–cyclam adduct and 2H9J for the Ni_2–xylylbicyclam adduct.

Acknowledgements

We thank the EPSRC (studentship for TMH), Wellcome Trust (Edinburgh Protein Interaction Centre) and RCUK (RASOR Interdisciplinary Research Centre in Proteomic Technologies) for their support for this work.

[1] X. Liang, P. J. Sadler, *Chem. Soc. Rev.* **2004**, *33*, 246–266.
[2] E. De Clercq, *Nat. Rev. Drug Discovery* **2002**, *1*, 13–25.

[3] E. De Clercq, N. Yamamoto, R. Pauwels, M. Baba, D. Schols, H. Nakashima, J. Balzarini, Z. Debyser, B. A. Murrer, D. Schwartz, D. Thornton, G. Bridger, S. Fricker, G. Henson, M. Abrams, D. Picker, *Proc. Natl. Acad. Sci. USA* **1992**, *89*, 5286–5290.
[4] G. J. Bridger, R. T. Skerlj, D. Thornton, S. Padmanabhan, S. A. Martellucci, G. W. Henson, M. J. Abrams, N. Yamamoto, K. De Vreese, R. Pauwels, E. De Clercq, *J. Med. Chem.* **1995**, *38*, 366–378.
[5] E. De Clercq, *Mol. Pharmacol.* **2000**, *57*, 833–839.
[6] E. Kimura, *Tetrahedron* **1992**, *48*, 6175–6217.
[7] J. A. Este, C. Cabrera, E. De Clercq, S. Struyf, J. Van Damme, G. Bridger, R. T. Skerlj, M. J. Abrams, G. Henson, A. Gutierrez, B. Clotet, D. Schols, *Mol. Pharmacol.* **1999**, *55*, 67–73.
[8] B. Bosnich, C. K. Poon, M. L. Tobe, *Inorg. Chem.* **1965**, *4*, 1102–1108.
[9] P. J. Connolly, E. J. Billo, *Inorg. Chem.* **1987**, *26*, 3224–3226.
[10] T. M. Hunter, S. J. Paisey, H. S. Park, L. Cleghorn, A. Parkin, S. Parsons, P. J. Sadler, *J. Inorg. Biochem.* **2004**, *98*, 713–719.
[11] X. Liang, M. Weishäupl, J. A. Parkinson, S. Parsons, P. A. McGregor, P. J. Sadler, *Chem. Eur. J.* **2003**, *9*, 4709–4717.
[12] X. Liang, J. A. Parkinson, M. Weishäupl, R. O. Gould, S. J. Paisey, H.-S. Park, T. M. Hunter, C. A. Blindauer, S. Parsons, P. J. Sadler, *J. Am. Chem. Soc.* **2002**, *124*, 9105–9112.
[13] L. O. Gerlach, J. S. Jakobsen, K. P. Jensen, M. R. Rosenkilde, R. T. Skerlj, U. Ryde, G. Bridger, T. W. Schwartz, *Biochemistry* **2003**, *42*, 710–717.
[14] T. M. Hunter, I. W. McNae, X. Liang, J. Bella, S. Parsons, M. D. Walkinshaw, P. J. Sadler, *Proc. Natl. Acad. Sci. USA* **2005**, *102*, 2288–2292.
[15] R. C. Holz, E. A. Evdokimov, F. T. Gobena, *Inorg. Chem.* **1996**, *35*, 3808–3814.
[16] E. K. Barefield, G. M. Freeman, D. G. Van Derveer, *Inorg. Chem.* **1986**, *25*, 552–558.
[17] D. T. Pierce, T. L. Hatfield, E. J. Billo, Y. Ping, *Inorg. Chem.* **1997**, *36*, 2950–2955.
[18] E. J. Billo, *Inorg. Chem.* **1981**, *20*, 4019–4021.
[19] R. J. Pell, H. W. Dodgen, J. P. Hunt, *Inorg. Chem.* **1983**, *22*, 529–532.
[20] Y. Dong, S. Farquhar, K. Gloe, L. F. Lindoy, B. R. Rumbel, P. Turner, K. Wichmann, *Dalton Trans.* **2003**, 1558–1566.
[21] Y. Dong, G. A. Lawrance, L. F. Lindoy, P. Turner, *Dalton Trans.* **2003**, 1567–1576.
[22] L. P. Battaglia, A. Bianchi, A. B. Corradi, E. Garciaespana, M. Micheloni, M. Julve, *Inorg. Chem.* **1988**, *27*, 4174–4179.
[23] J. W. Cai, C.-H. Che, J. S. Zhou, *Wuji Huaxue Xuebao (Chin. J. Inorg. Chem.)* **2003**, *19*, 81–85.
[24] S. J. Li, A. Nakagawa, T. Tsukihara, *Biochem. Biophys. Res. Commun.* **2004**, *324*, 529–533.
[25] S. J. Li, *Biopolymers* **2006**, *81*, 74–80.
[26] C. Li, W.-T. Wong, *Tetrahedron Lett.* **2002**, *43*, 3217–3220.
[27] SADABS: G. M. Sheldrick, University of Göttingen (Germany), **2004**.
[28] A. Altomare, G. Cascarano, C. Giacovazzo, A. Guagliardi, *J. Appl. Crystallogr.* **1993**, *26*, 343–350.
[29] SHELXS-97: G. M. Sheldrick, University of Göttingen (Germany), **1997**.
[30] P. T. Beurskens, G. Beurskens, W. P. Bosman, R. de Gelder, S. Garcia Granda, R. O. Gould, R. Israel, J. M. M. Smits, Crystallography Laboratory, University ofNijmegen (The Netherlands), **1996**.
[31] P. W. Betteridge, J. R. Carruthers, R. I. Coopers, K. Prout, D. J. Watkin, *J. Appl. Crystallogr.* **2003**, *36*, 1487.
[32] SHELXL-97: G. M. Sheldrick,, University of Göttingen (Germany), **1997**.
[33] A. G. W. Leslie, *Joint CCP4 + ESF-EAMCB Newsletter on Protein Crystallography* **1992**, 26.
[34] Collaborative Computational Project, Number 4, *Acta Crystallogr. Sect. D* **1994**, *50*, 760–763.
[35] G. N. Murshudov, A. A. Vagin, E. J. Dodson, *Acta Crystallogr. Sect. D* **1997**, *53*, 240–255.
[36] P. Emsley, K. Cowtan, *Acta Crystallogr. Sect. D* **2004**, *60*, 2126–2132.
[37] The Protein Data Bank: H. M. Berman, J. Westbrook, Z. Feng, G. Gilliland, T. N. Bhat, H. Weissig, I. N. Shindyalov, P. E. Bourne, *Nucleic Acids Res.* **2000**, *28*, 235–242.

Received: September 15, 2006
Published online: November 22, 2006

